

A VUV Photoionization Study of the Combustion-Relevant Reaction of the Phenyl Radical (C_6H_5) with Propylene (C_3H_6) in a High Temperature Chemical Reactor

Fangtong Zhang and Ralf I. Kaiser*

Department of Chemistry, University of Hawaii at Manoa, Honolulu, Hawaii 96822, United States

Amir Golan and Musahid Ahmed*

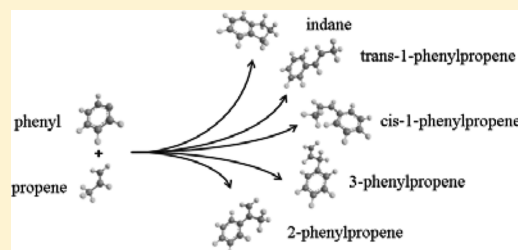
Chemical Sciences Division, Lawrence Berkeley National Laboratory, Berkeley, California 94720, United States

Nils Hansen

Combustion Research Facility, Sandia National Laboratories, Livermore, California 94551, United States

Supporting Information

ABSTRACT: We studied the reaction of phenyl radicals (C_6H_5) with propylene (C_3H_6) exploiting a high temperature chemical reactor under combustion-like conditions (300 Torr, 1200–1500 K). The reaction products were probed in a supersonic beam by utilizing tunable vacuum ultraviolet (VUV) radiation from the Advanced Light Source and recording the photoionization efficiency (PIE) curves at mass-to-charge ratios of $m/z = 118$ ($C_9H_{10}^+$) and $m/z = 104$ ($C_8H_8^+$). Our results suggest that the methyl and atomic hydrogen losses are the two major reaction pathways with branching ratios of $86 \pm 10\%$ and $14 \pm 10\%$. The isomer distributions were probed by fitting the recorded PIE curves with a linear combination of the PIE curves of the individual C_9H_{10} and C_8H_8 isomers. Styrene ($C_6H_5C_2H_3$) was found to be the *exclusive* product contributing to $m/z = 104$ ($C_8H_8^+$), whereas 3-phenylpropene, *cis*-1-phenylpropene, and 2-phenylpropene with branching ratios of $96 \pm 4\%$, $3 \pm 3\%$, and $1 \pm 1\%$ could account for the signal at $m/z = 118$ ($C_9H_{10}^+$). Although searched for carefully, no evidence of the bicyclic indane molecule could be provided. The reaction mechanisms and branching ratios are explained in terms of electronic structure calculations nicely agreeing with a recent crossed molecular beam study on this system.



1. INTRODUCTION

As precursors of soot as well as their importance in combustion,^{1–3} atmospheric,^{4,5} and interstellar chemistry,^{6,7} the formation routes to polycyclic aromatic hydrocarbons (PAHs) have received considerable attention.^{8,9} It is widely accepted that the phenyl radical, $C_6H_5(X^2A_1)$, represents a crucial building block to yield the second ring, thus initiating the formation of PAHs and related molecules such as (partially) hydrogenated and/or dehydrogenated PAHs in combustion systems.^{10–12} In detail, PAHs have been suggested to be formed via hydrogen abstraction–acetylene addition (HACA) sequences¹³ or via phenyl addition–cyclization pathways (PAC).¹⁴ Alternative pathways have been investigated via kinetic studies^{15–18} and crossed beam experiments^{19–22} of phenyl radicals with unsaturated hydrocarbons. Very recently, indane has been identified as one of the products in a low-pressure premixed toluene/oxygen/argon fuel rich flame by Li et al. in 2009.²³ The aromatic, bicyclic indane molecule as well as its α -methylstyrene (2-phenylpropene) and 1-phenylpropene isomers are considered important reaction intermediates and

toxic byproducts in the combustion of fossil fuel (Figure 1).^{10,11,23–27} The reaction of the phenyl radical (C_6H_5) with propylene (C_3H_6) presents a potential synthetic route to synthesize C_9H_{10} isomers and to access the C_9H_{11} potential energy surface.

As early as in 1972, Hefter et al.²⁸ investigated this system in liquid propylene at 183 K utilizing electron spin resonance. In 2006, Park et al.¹⁶ conducted a kinetics study exploiting cavity ring-down spectroscopy at temperatures between 296 and 496 K combined with *ab initio* calculations; in 2008, Kaiser et al. conducted a crossed beam experiment of this system at elevated collision energies of 130–190 kJ mol⁻¹.²⁰ All three studies agreed that this reaction was initiated by an addition of the phenyl radical predominantly to the C1-carbon atom of the propylene molecule at the =CH₂ unit to form a doublet radical intermediate; the latter ejected a hydrogen atom via a

Received: January 26, 2012

Revised: February 29, 2012

Published: March 6, 2012

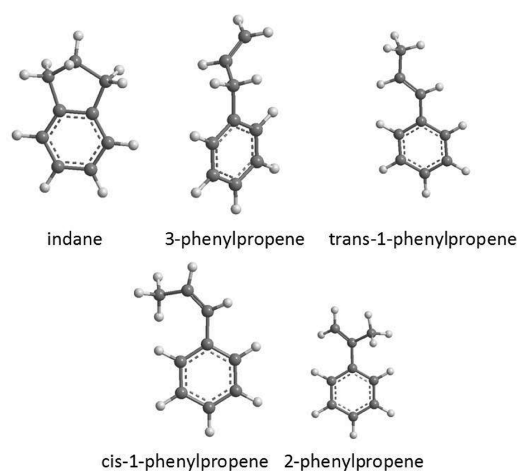


Figure 1. Structures of distinct C₉H₁₀ isomers potentially formed in the reaction of phenyl radicals with propylene.

rather loose exit transition state, forming solely monocyclic C₉H₁₀ isomers. No methyl group loss was observed at elevated collision energies. Most recently, our group reinvestigated this reaction, utilizing a crossed beam method at a much lower collision energy of about 45 kJ mol⁻¹.²⁹ The methyl group loss channel yielding styrene was successfully identified, and a fraction of the methyl versus hydrogen loss channels of 68 ± 6% to 32 ± 10% was derived experimentally, agreeing nicely with RRKM theory. Apart from the crossed beam,^{19–21,30} flame,^{9,31} and shock tube^{32–34} studies, reactions carried out under pyrolytic conditions present an excellent complementary approach to simulate combustion-like conditions and to investigate the formation mechanisms of PAHs.³⁵ In 2008, Shukla et al.¹⁴ conducted an investigation on the basis of a kinetic analysis of gas phase products of pyrolysis of benzene with and without addition of acetylene. Reactions were conducted in a flow tube, and the products were probed in situ by a *direct sampling* mass spectrometric technique using vacuum ultraviolet (VUV) single photon ionization (SPI) time-of-flight mass spectrometry (TOF-MS). The authors found that the PAC pathway presented a highly efficient growth mechanism to form PAHs. The products included PAHs up to 454 amu (C₃₆H₂₂). Especially, acetylene was mixed with benzene to understand the impact of HACA on the PAC pathways; this resulted in an enhancement of PAH production in spite of trapping of active and chain-carrier species such as the phenyl radical by acetylene to form phenylacetylene. The comparison of both the HACA and PAC mechanisms concluded that PAC is a highly efficient mechanism for the growth of PAHs.

Recently, we studied the reaction of phenyl (C₆H₅) with methylacetylene (CH₃CCH) and allene (H₂CCCH₂) by exploiting a high temperature chemical reactor under combustion-like conditions (300 Torr, 1200–1500 K).³⁶ The product isomer distributions were probed utilizing tunable VUV radiation from the Advanced Light Source (ALS) by recording the photoionization efficiency (PIE) curves at a mass-to-charge of $m/z = 116$ (C₉H₈⁺) of the products in a supersonic expansion. Branching ratios were derived by fitting the recorded PIE curves with a linear combination of the individual C₉H₈ isomer PIE curves. In both reactions, the aromatic indene molecule was identified. In this paper we expand on these studies systematically by decreasing the carbon-to-hydrogen

ratio of the closed shell reactant from 0.75 (methylacetylene, allene) to 0.5 (propylene) and report on the results of the phenyl-propene reaction utilizing the very same pyrolytic reactor. Recall that in case of distinct structural isomers, the adiabatic ionization energy (IE) and the corresponding PIE curves, which report the ion signal of $m/z = 118$ (C₉H₁₀⁺) of a distinct isomer versus the photon energy, can differ dramatically. By photoionizing the neutral C₉H₁₀ products in the supersonic molecular beam via tunable vacuum ultraviolet (VUV) radiation from the Advanced Light Source at various photon energies, we measured PIEs of $m/z = 118$ (C₉H₁₀⁺) and $m/z = 104$ (C₈H₈⁺). These PIE curves are the result of a linear combination of the individual isomer PIE curves present in the supersonic beam and hence we can identify the products formed in the reactions of phenyl radicals with propylene and extract their branching ratios.

2. EXPERIMENTAL SECTION

The central device of the experiments is a resistively heated high temperature “chemical reactor”³⁷ incorporated into the molecular beams end station at the Chemical Dynamics Beamline (9.0.2.) of the Advanced Light Source. Briefly, this setup allows a simulation of combustion-relevant conditions such as temperature and pressure as well as chemical reactions to form combustion-relevant molecules such as PAHs and their isomers in situ. Here, a continuous beam of phenyl radicals (C₆H₅) was generated in situ via quantitative pyrolysis of nitrosobenzene (C₆H₅NO; Aldrich) (held at 293 K) seeded in neat propylene carrier gas (C₃H₆; Sigma), which was expanded at a pressure of 300 Torr through a 0.1 mm orifice into a resistively heated silicon carbide (SiC) tube with an inner diameter of 1 mm and a length of 20 mm. A heating current of 1.3 A was applied to the silicon carbide tube reflecting an operating power of 20 W. An independent temperature calibration of the pyrolytic source with pure helium carrier gas coupled to a time-of-flight mass spectrometer and chopper wheel suggested temperatures of 1200–1500 K of the silicon carbide tube. In the present experiments, we would like to stress that propylene acted not only as a seeding gas but also as a reactant with the pyrolytically generated phenyl radicals. Considering the length of the tube of 2.0 ± 0.1 cm and a thermal, nonsupersonic velocity of the propylene reactant at 1350 ± 150 K inside the tube of 900 ± 50 ms⁻¹, we estimate a residence time of the reactants in the silicon carbide tube of 24 ± 2 μs. The setup allows an analysis of the in situ generated products. Here, after passing a 2-mm-diameter skimmer located 10 mm downstream from the silicon carbide nozzle, quasi continuous tunable VUV radiation from the ALS crossed the neutral molecular beam at the extraction region of a Wiley–McLaren reflectron time-of-flight (Re-TOF) mass spectrometer 55 mm downstream. The ions of the photoionized molecules were then extracted and collected by a microchannel plate detector in the Re-TOF mode utilizing a multichannel scaler. The PIE curves were obtained by plotting the integrated relevant ion counts at a desired mass-to-charge, m/z , versus the photoionization energy between 8.0 and 10.1 eV in steps of 0.1 eV. The signal was normalized to the photon flux. On the basis of calibrated PIE curves of expected products of a well-defined molecular mass and their acyclic isomers ($m/z = 118$; C₉H₁₀), the recorded PIE curves were then fit via a linear combination with known PIE curves of various C₉H₁₀ isomers to extract the nature of the products formed and their branching ratios.

To fit the PIE curve at $m/z = 118$ (C_9H_{10}) obtained during the phenyl–propylene experiment, we also recorded the PIE curves of the individual C_9H_{10} isomers, which are not available from the literature (Supporting Information) (Figure 1). Briefly, the PIE curves of five C_9H_{10} isomers indane (TCI, 98%), 3-phenylpropene (TCI, 98%), *cis/trans*-1-phenylpropene (TCI, 98%), and α -methylstyrene (2-phenylpropene) (Sigma Aldrich, 98%) were recorded also at the Chemical Dynamics Beamline (9.0.2.) of the Advanced Light Source. For each isomer, a continuous beam of the C_9H_{10} isomer was generated by passing helium (Airgas, 99.999%) carrier gas with a pressure of 300 Torr through a homemade stainless steel bubbler, which contained the individual C_9H_{10} isomer at 293 K. This gas mixture expanded through a 0.1 mm orifice into the source chamber before passing a 2-mm-diameter skimmer 10 mm downstream to reach the detector chamber. As for the reaction products, the ions of the photoionized molecules were then extracted and collected by a microchannel plate detector in the Re-TOF mode. Individual PIE curves were obtained by plotting the integrated ion counts $m/z = 118$ versus the photoionization energy between 8.00 and 10.10 eV in steps of 0.025 or 0.01 eV. The signal was normalized to the photon flux. The PIE curves of the five C_9H_{10} isomers are presented in the Supporting Information. The ionization energies were derived to be 8.42, 8.40, 8.28, 8.38, and 8.23 eV for indane, 3-phenylpropene, *cis/trans*-1-phenylpropene, and α -methylstyrene, respectively. These values can be compared with NIST data of 8.45, 8.2–8.7, 8.5, 8.3, and 8.3, respectively.³⁸

3. RESULTS AND DISCUSSION

The mass spectra of the species formed in the supersonic expansion and the PIE curves of $m/z = 118$ ($C_9H_{10}^+$) and $m/z = 104$ ($C_8H_8^+$) are shown in Figures 2 and 3, respectively.

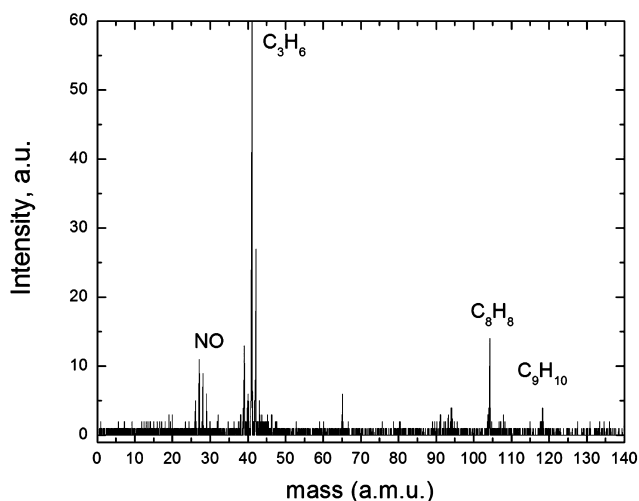


Figure 2. Mass spectrum of the products of the phenyl–propene pyrolytic reaction recorded at a photon energy of 8.6 eV. Note that the mass spectrum of the nonpyrolyzed gas mixture depicted ion counts for both propylene ($m/z = 42$) and nitrosobenzene ($m/z = 107$).

Apart from the signal at $m/z = 30$ (NO) and $m/z = 42$ (C_3H_6), the mass spectrum depicts peaks at $m/z = 104$ and 118 corresponding to $C_8H_8^+$ and $C_9H_{10}^+$, respectively. These products are formed via the methyl and hydrogen loss channels, respectively, in the reaction of phenyl radicals with propylene (eqs 1 and 2). The branching ratios of both channels

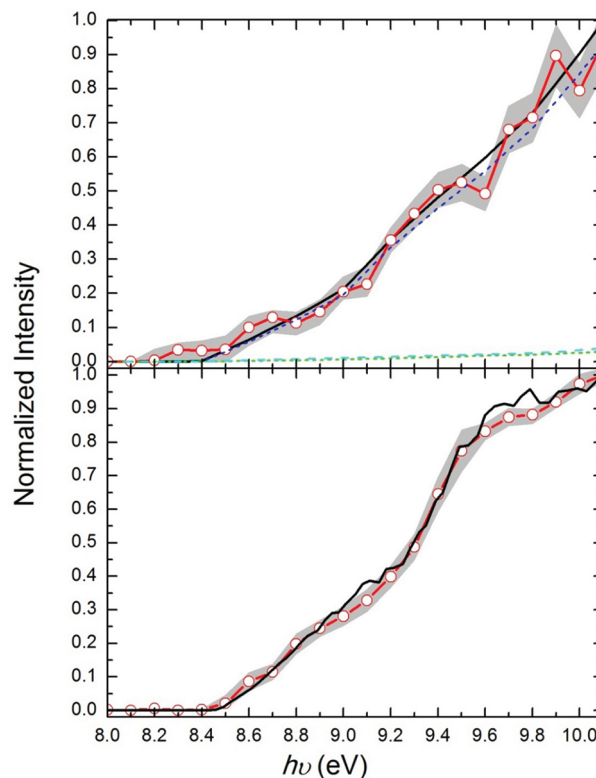
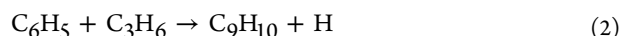


Figure 3. Upper panel: red circles and line present the PIE obtained at $m/z = 118$, whereas the black line is the simulation using PIEs of 3-phenylpropene (blue), *cis*-1-phenylpropene (green), and 2-phenylpropene (cyan). Lower panel: red circles and line present the PIE obtained at $m/z = 104$; the PIE curve of styrene is taken from ref 39. Experimental errors are defined by the gray curve.

are estimated from the peak intensities and scaled photon absorption cross sections³⁹ to be about $86 \pm 10\%:14 \pm 10\%$.



Note that the peak at $m/z = 94$ might correspond to phenol, which is likely produced in the reactions involving the nitrogen monoxide byproduct formed in the pyrolysis of nitrosobenzene.

As discussed above, the major products of the phenyl–propene reaction hold the molecular formulas C_8H_8 and C_9H_{10} . We attempt now to fit the recorded PIEs with a linear combination of PIEs of the corresponding isomers. The PIE curve of $m/z = 104$ (C_8H_8) can be reproduced exclusively with the literature PIE curve of styrene ($C_6H_5C_2H_3$). The experimentally recorded PIE curve of $m/z = 118$ (C_9H_{10}) can be principally fit with the PIE of the 3-phenylpropene isomer. Fractions of *cis*-1-phenylpropene and 2-phenylpropene at the few percent level slightly improve the fit with an overall branching ratio of 3-phenylpropene, *cis*-1-phenylpropene, and 2-phenylpropene of $96 \pm 4\%$, $3 \pm 3\%$, and $1 \pm 1\%$. Noticeably, there is no evidence of the formation of the bicyclic indane molecule. This is in contrary to the phenyl–allene/propyne reactions, in which the bicyclic indene molecule was identified.³⁶

In an attempt to understand the predominant formation of 3-phenylpropene and styrene, we inspected the underlying potential energy surface (PES).²⁹ As predicted computationally, the phenyl–propene reaction is likely initiated by the phenyl

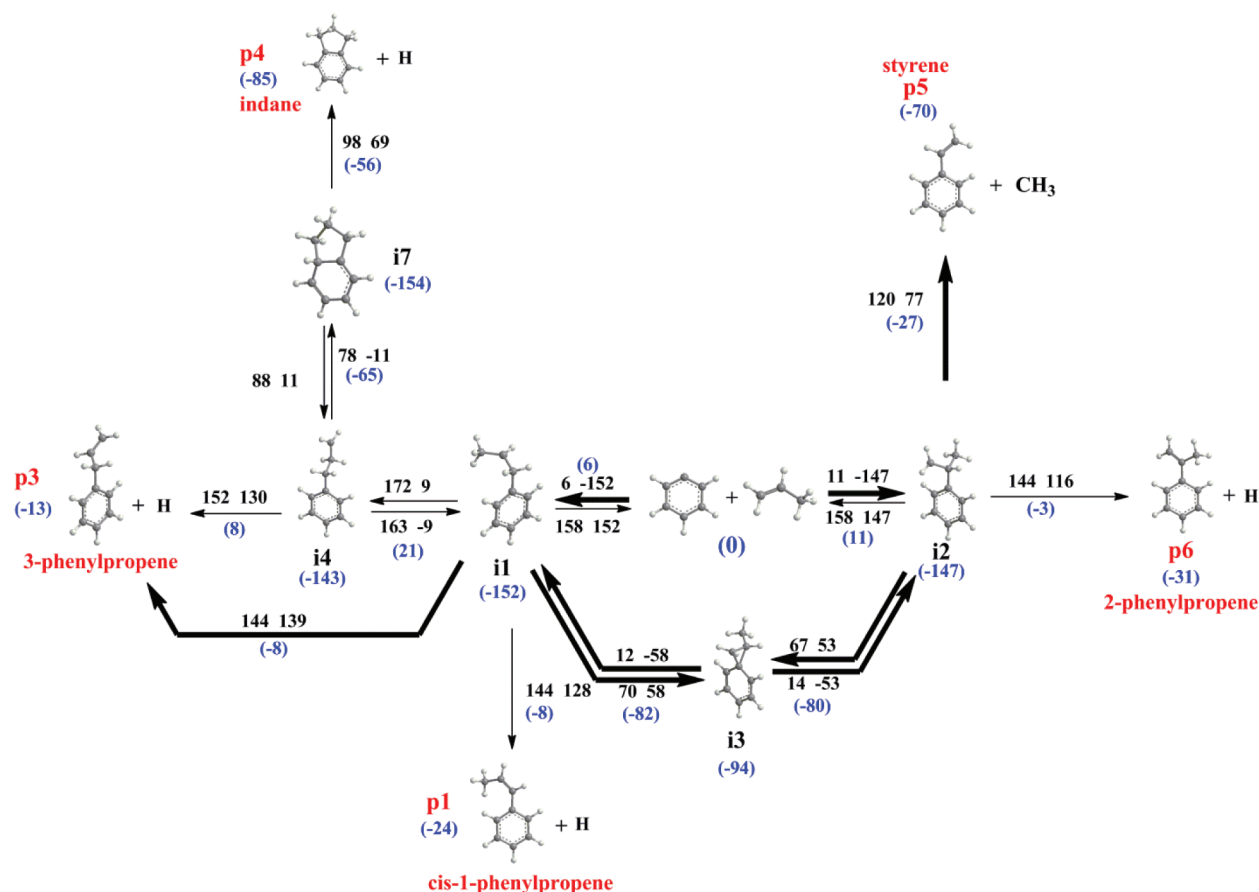


Figure 4. Relevant parts of the potential energy surface of the phenyl plus propene reaction taken from ref 29. All relative energies (shown in blue color online and in parentheses, in kJ mol^{-1}) are calculated at the G3(MP2,CC)//B3LYP/6-311G(d,p) + ZPE(B3LYP/6-311G(d,p)) level of theory. The numbers next to the arrows show the barrier (first) and the reaction energy (second) for each individual step in kJ mol^{-1} .

addition of the phenyl radical with its unpaired electron to the sterically less hindered CH_2 group of the propylene molecule to form the **i1** intermediate located 152 kJ mol^{-1} below the reactants via a 6.3 kJ mol^{-1} barrier; alternatively, phenyl can add to the CH group of propylene, yielding the **i2** intermediate, which is almost isoenergetic to **i1** and placed 147 kJ mol^{-1} below the reactants via a higher 11.3 kJ mol^{-1} barrier. Both **i1** and **i2** intermediates are interconvertible via intermediate **i3**. Intermediate **i1** can eject a hydrogen atom from the methyl group to form the 3-phenylpropene product. This reaction channel is overall exoergic by 13 kJ mol^{-1} . From the **i2** intermediate, a methyl group can be ejected to yield the styrene product. Besides those two major reaction pathways highlighted via bold arrows in Figure 4, two minor pathways were identified. First, **i1** can lose a hydrogen atom from the adjacent CH_2 group to form *cis*-1-phenylpropene molecule; this channel is exoergic by 24 kJ mol^{-1} . Further, **i2** can emit atomic hydrogen and form 2-phenylpropene. It can be seen that to access the bicyclic indane molecule, the reaction has to go through a multistep pathway involving **i1** \rightarrow **i4** \rightarrow **i7** \rightarrow indane + H. More importantly, the barrier between **i1** and **i4** is located 21 kJ mol^{-1} above the reactants. Due to this barrier, the pathway to form indane is less likely than yielding 3-phenylpropene and styrene. Also, intermediate **i1** is critical to form indane. However, considering the barriers for the competing pathways **i1** might follow, **i1** rather fragments to 3-phenylpropene plus atomic hydrogen instead of pursuing the reaction sequence **i1** \rightarrow **i4** \rightarrow **i7** \rightarrow indane plus hydrogen. This

reaction scheme correlates well with our experimental results, in which styrene and 3-phenylpropene are identified as the two major products, as well as the *cis*-1-phenylpropene and 2-phenylpropene molecules possibly existing at small fractions at the percent level. Also, no indane molecule was observed. Compared to the recent crossed beam reaction, of phenyl with propylene,²⁹ the results also agree very nicely. First, the branching ratios of the methyl and hydrogen loss pathways were determined to be $68 \pm 16\%$ and $32 \pm 10\%$, respectively, under single collision conditions at a collision energy of about 45 kJ mol^{-1} . Further, the crossed beam reaction did not depict any evidence of indane formation.

We highlight that little is known about the combustion chemistry of the phenyl-propene system. As a matter of fact, although the reaction product styrene has been detected in combustion flames, the 3-phenylpropene molecule, formed via the phenyl radical-atomic hydrogen replacement pathway, has not been included in any of the commonly used combustion chemistry models. Nevertheless, these species could contribute to molecular-weight growth in combustion processes: hydrogen-abstraction reactions from the experimentally observed phenylpropene isomers provide conceivable pathways to phenyl-substituted allyl radicals: 1-phenylallyl and 2-phenylallyl. Similar to benzene and fulvene formation via the propargyl-allyl or allyl-allyl reactions, phenyl-substituted allyl radicals could provide pathways to biphenyl or triphenyl involving reactions with propargyl (or allyl) or phenyl-substituted allyl radicals. Likewise, hydrogen atoms as present in combustion

flames, might change the spectrum of the primary reaction products and could lead via hydrogen addition–isomerization–hydrogen elimination to the indane molecule. Alternatively, the indane molecule as observed in combustion flames might be formed via hydrogenation of indene, with the latter being formed in the phenyl–allene and phenyl–methylacetylene reactions.

4. CONCLUSIONS

We investigated the combustion-relevant reaction of phenyl radicals (C_6H_5) with propylene (C_3H_6) by exploiting a high temperature chemical reactor under combustion-like conditions at temperatures of about 1200–1500 K. The reaction products were probed in a supersonic beam by utilizing tunable VUV radiation from the Advanced Light Source and recording the PIE curves at mass-to-charge ratios of $m/z = 118$ ($C_9H_{10}^+$) and $m/z = 104$ ($C_8H_8^+$). Our results indicate that the methyl and atomic hydrogen losses are the two major reaction pathways with branching ratios of $86 \pm 10\%$ and $14 \pm 10\%$. Styrene ($C_6H_5C_2H_3$) was found to be the *exclusive* product contributing to $m/z = 104$ ($C_8H_8^+$), whereas 3-phenylpropene, *cis*-1-phenylpropene, and 2-phenylpropene with branching ratios of $96 \pm 4\%$, $3 \pm 3\%$, and $1 \pm 1\%$ could account for signal at $m/z = 118$ ($C_9H_{10}^+$). No evidence of the bicyclic indane molecule could be provided. These isomers could contribute to molecular-weight growth in combustion processes because hydrogen-abstraction reactions from the phenylpropene isomers provide viable pathways to phenyl-substituted allyl radicals. These are 1-phenylallyl and 2-phenylallyl. These phenyl-substituted allyl radicals could provide pathways to biphenyl or triphenyl involving reactions with propargyl (or allyl) or phenyl-substituted allyl radicals.

■ ASSOCIATED CONTENT

Supporting Information

Photoionization efficiency curves (PIEs) of the calibrated C_9H_{10} isomers tabulated in ascii form. This information is available free of charge via the Internet at <http://pubs.acs.org>.

■ AUTHOR INFORMATION

Notes

The authors declare no competing financial interest.

■ ACKNOWLEDGMENTS

This research was supported by the US Department of Energy Office of Science via project DE-FG02-03-ER15411 (RIK, FZ). M.A. and A.G. are supported by the Office of Science, Office of Basic Energy Sciences, of the US Department of Energy under Contract No. DE-AC02-05CH11231, through the Chemical Sciences Division. The Advanced Light Source is supported by the Director, Office of Science, Office of Basic Energy Sciences, of the U.S. Department of Energy under Contract No. DE-AC02-05CH11231. Sandia is a multiprogram laboratory operated by Sandia Corporation, a Lockheed Martin Co., for the National Nuclear Security Administration under contract DE-AC04-94-AL85000.

■ REFERENCES

- (1) Goldaniga, A.; Faravelli, T.; Ranzi, E. *Combust. Flame* **2000**, *122*, 350–358.
- (2) Marinov, N. M.; Pitz, W. J.; Westbrook, C. K.; Castaldi, M. J.; Senkan, S. M. *Combust. Sci. Technol.* **1996**, *116–117*, 211–287.

- (3) Sye, W. F.; Lin, C. L.; Yen, D. P.; Tsai, C. S. *J. Chin. Chem. Soc. (Taipei)* **1988**, *35*, 1–11.
- (4) Ergut, A.; Levendis, Y. A.; Richter, H.; Carlson, J. *Fourth Joint Meeting of the U.S. Sections of the Combustion Institute*; Combustion Institute: Philadelphia, PA, 2005; A05/1–6.
- (5) Atkinson, R.; Arey, J. *Environ. Health Perspect. Suppl.* **1994**, *102*, 117–126.
- (6) Wakelam, V.; Herbst, E. *Astrophys. J.* **2008**, *680*, 371–383.
- (7) Helling, C.; Joergensen, U. G.; Plez, B.; Johnson, H. R. *Astron. Astrophys.* **1996**, *315*, 194–203.
- (8) Frenklach, M.; Feigelson, E. D. *Astrophys. J.* **1989**, *341*, 372–384.
- (9) Richter, H.; Howard, J. B. *Prog. Energy Combust. Sci.* **2000**, *26*, 565–608.
- (10) Lindstedt, P.; Maurice, L.; Meyer, M. *Faraday Discuss.* **2002**, *119*, 409–432; discussion 445–459
- (11) Kamphus, M.; Braun-Unkoff, M.; Kohse-Hoinghaus, K. *Combust. Flame* **2008**, *152*, 28–59.
- (12) Frenklach, M. *Phys. Chem. Chem. Phys.* **2002**, *4*, 2028–2037.
- (13) Bockhorn, H.; Fetting, F.; Heddrich, A.; Wannemacher, G. *Ber. Bunsen-Ges. Phys. Chem.* **1987**, *91*, 819–825.
- (14) Shukla, B.; Susa, A.; Miyoshi, A.; Koshi, M. *J. Phys. Chem. A* **2008**, *112*, 2362–2369.
- (15) Yu, T.; Lin, M. C. *Combust. Flame* **1995**, *100*, 169–176.
- (16) Park, J.; Nam, G. J.; Tokmakov, I. V.; Lin, M. C. *J. Phys. Chem. A* **2006**, *110*, 8729–8735.
- (17) Tokmakov, I. V.; Park, J.; Lin, M. C. *ChemPhysChem* **2005**, *6*, 2075–2085.
- (18) Park, J.; Wang, L.; Lin, M. C. *Int. J. Chem. Kinet.* **2003**, *36*, 49–56.
- (19) Gu, X.; Kaiser, R. I. *Acc. Chem. Res.* **2009**, *42*, 290–302.
- (20) Zhang, F.; Gu, X.; Guo, Y.; Kaiser, R. I. *J. Phys. Chem. A* **2008**, *112*, 3284–3290.
- (21) Zhang, F.; Gu, X.; Guo, Y.; Kaiser, R. I. *J. Org. Chem.* **2007**, *72*, 7597–7604.
- (22) Gu, X.; Zhang, F.; Guo, Y.; Kaiser, R. I. *Angew. Chem., Int. Ed.* **2007**, *46*, 6866–6869.
- (23) Li, Y.; Zhang, L.; Tian, Z.; Yuan, T.; Wang, J.; Yang, B.; Qi, F. *Energy Fuels* **2009**, *23*, 1473–1485.
- (24) Newby, J. J.; Stearns, J. A.; Liu, C.-P.; Zwier, T. S. *J. Phys. Chem. A* **2007**, *111*, 10914–10927.
- (25) Li, Y.; Tian, Z.; Zhang, L.; Yuan, T.; Zhang, K.; Yang, B.; Qi, F. *Proc. Combust. Inst.* **2009**, *32*, 647–655.
- (26) Li, Y.; Zhang, L.; Yuan, T.; Zhang, K.; Yang, J.; Yang, B.; Qi, F.; Law, C. K. *Combust. Flame* **2010**, *157*, 143–154.
- (27) Richter, H.; Howard, J. B. *Prog. Energy Combust. Sci.* **2000**, *26*, 565–608.
- (28) Hefter, H. J.; Hecht, T. A.; Hammond, G. S. *J. Am. Chem. Soc.* **1972**, *94*, 2793–2797.
- (29) Kaiser, R. I.; Parker, D. S. N.; Goswami, M.; Zhang, F.; Kislov, V. V.; Mebel, A. M.; Aguilera-Iparraguirre, J.; Green, W. H. *Phys. Chem. Chem. Phys.* **2011**, *14*, 720–729.
- (30) Gu, X.; Guo, Y.; Mebel, A. M.; Kaiser, R. I. *Chem. Phys. Lett.* **2007**, *449*, 44–52.
- (31) Hansen, N.; Klippenstein, S. J.; Westmoreland, P. R.; Kasper, T.; Kohse-Hoinghaus, K.; Wang, J.; Cool, T. A. *Phys. Chem. Chem. Phys.* **2008**, *10*, 366–374.
- (32) Wang, H. *Int. J. Chem. Kinet.* **2001**, *33*, 698–706.
- (33) Bentz, T.; Giri, B. R.; Hippler, H.; Olzmann, M.; Striebel, F.; Szoeri, M. *J. Phys. Chem. A* **2007**, *111*, 3812–3818.
- (34) Kern, R. D.; Xie, K.; Chen, H. *Combust. Sci. Technol.* **1992**, *85*, 77–86.
- (35) Yuan, T.; Zhang, L.; Zhou, Z.; Xie, M.; Ye, L.; Qi, F. *J. Phys. Chem. A* **2011**, *115*, 1593–1601.
- (36) Zhang, F.; Kaiser, R. I.; Kislov, V. V.; Mebel, A. M.; Golan, A.; Ahmed, M. *J. Phys. Chem. Lett.* **2011**, *2*, 1731–1735.
- (37) Kohn, D. W.; Claiberg, H.; Chen, P. *Rev. Sci. Instrum.* **1992**, *63*, 4003–4005.
- (38) Linstrom, P. J.; Mallard, W. G. *NIST Chemistry WebBook*; NIST: Gaithersburg, MD, 2005.

(39) Zhou, Z.; Xie, M.; Wang, Z.; Qi, F. *Rapid Commun. Mass Spectrom.* **2009**, *23*, 3994–4002.